Research Square

Preprints are preliminary reports that have not undergone peer review.
They should not be considered conclusive, used to inform clinical practice,
or referenced by the media as validated information.

Computing shared charging equilibria under heterogeneous fuzzy preferences

Yinpu Ma

mayinpu@163.com

North Minzu University

Cunlin Li

North Minzu University

Research Article

Keywords:

Posted Date: November 25th, 2026

DOI: https://doi.org/10.21203/rs.3.rs-11560420/v1

License: This work is licensed under a Creative Commons Attribution 4.0 International License.
Read Full License

Additional Declarations: No competing interests reported.

Computing shared charging equilibria under heterogeneous fuzzy preferences

Yinpu Ma[1] and Cunlin Li[1*]

[1]School of Mathematics and Information Science,North Minzu University,Yinchuan,750021,Ningxia,China.

*Corresponding author(s). E-mail(s): 349257568@qq.com;
Contributing authors: mayinpu@163.com;

Abstract

Drone fleet operators sharing charging capacity may assign different priorities to lower, modal and upper congestion costs. We study a continuous reservation game in which these declared triangular preferences generate heterogeneous quadratic congestion coefficients. The selected solution is a variational generalized Nash equilibrium with a common capacity multiplier. For independent reservation periods, we derive a capacity test that separates aggregate consistency from price clearing. Each branch is a scalar monotone equation, giving a unique equilibrium allocation without requiring monotonicity of the full pseudogradient. Active set formulas describe how an operator's congestion coefficient changes its reservation and the reservations of its competitors. An aggregate and price bisection implementation is checked against exhaustive complementarity enumeration on 90 small cases. Thirty new scaling instances with up to 2048 operators and six periods compare this implementation with extragradient on the same game. Median paired speed ratios range from 25.7 to 44.3, while a separate comparison uses a KKT least squares implementation. Best response experiments show that negligible unilateral regret can coexist with a large variational inequality gap. All results use archived synthetic inputs. The computation exploits a separable aggregative structure; it does not establish a new general fuzzy ranking principle, solve aircraft routing, or validate battery operation.

Keywords: Generalized Nash equilibrium, shared charging capacity, triangular fuzzy preferences, aggregative games, equilibrium verification

1 Introduction

Sharing charging infrastructure creates a strategic allocation problem before any aircraft route is executed. An operator seeking additional charging capacity changes both aggregate congestion and the residual capacity available to competitors. A centralized delivery schedule followed by a cost allocation does not describe this choice: here operators select their own continuous reservations, and participation is assessed through feasible unilateral deviations.

Uncertainty preferences add a second distinction. Operators may describe congestion costs by triangular numbers yet weight the endpoints differently. A declared linear score translates these descriptions into operator-specific deterministic coefficients. It is therefore necessary to identify which conclusions depend on preferences, which follow from the game structure, and which are supported by numerical certificates. In particular, a small unilateral deviation gain does not identify a common-price equilibrium when a shared capacity is binding.

The mathematical foundations are established. Shared-constraint games distinguish generalized Nash equilibria (GNEs) from variational equilibria (VEs) [1]. Nonsmooth gap reformulations can characterize all GNEs [2], and modern software exploits joint KKT systems for nonlinear and quadratic games [3]. Aggregative reductions and equilibrium uniqueness have a long history [4, 5]; exact algorithms also exist for broader resource allocation and Cournot classes [6]. Consequently, scalar aggregation, common multipliers and bisection are methodological foundations of this work, rather than new general principles.

We develop a specific connection between heterogeneous triangular preference scores and a capacity-constrained charging reservation game. Its useful feature is an explicit split: either the unconstrained aggregate fits within capacity, or the aggregate equals capacity and a scalar multiplier clears reservations. This split gives an auditable computation even when the full pseudogradient is nonmonotone. We additionally derive local preference sensitivities and verify separately primal feasibility, unilateral regret, the VI gap and common-price stationarity. These checks prevent a generic best response fixed point from being reported as the selected VE.

The contributions are: (i) a complete aggregate/price characterization and uniqueness proof for this separable capped game; (ii) active set formulas for the effect of a single congestion preference coefficient; (iii) an implementation with independent active set and projection checks; and (iv) new synthetic experiments distinguishing computational comparisons from changes in the game induced by different preferences. The claimed contribution is this model-specific characterization and reproducible verification package. We do not claim priority for aggregate response techniques or a general-purpose equilibrium algorithm.

Section 2 positions the model. Sections 3–4 define the game and establish the characterization. Section 5 gives the algorithms and certificates. Section 6 reports completed computations, followed by limitations in Section 7.

Table 1 Relationship to close methodological and application studies

Study	Established component	Scope of this paper
Itaya and von Mouche [5]	Aggregate response techniques and uniqueness	Capped common-price branches and explicit preference derivatives
Harks and Timmermans [6]	Exact resource allocation and Cournot algorithms	A narrower continuous model with independent periods
Bemporad [3]	General KKT computational framework	A local SciPy KKT baseline, not a reproduction of NashOpt
Yang et al. [10]	Budgeted consensus games and sequential verification	Charging reservations and a specified VE selection
Liu and Gong [14]	UAV facilities and cooperative allocation	No coalition characteristic function or post hoc cost sharing

2 Related research and scope

Preference relations for interval and fuzzy interval optimization support explicit distinctions between dominance and selection [7]. Urbanec's fuzzy order extensions [8] concern graded relations and underlying fuzzy equalities; they are not a license to identify every triangular scoring rule with a linear extension. We use an endpoint score, state its weights directly, and require no total-extension theorem.

The supplied GNE literature suggests both useful constructions and limits. Lampariello et al. [9] consider hierarchical equilibrium selection with nonsmooth terms, a substantially richer structure than independent reservation periods. Choi et al.'s supplied July 2026 arXiv revision treats quasi-linear polynomial games through partial multiplier expressions and moment relaxations; it seeks a different level of generality and, under stated conditions, all equilibria. It is a preprint and is mentioned here as such (arXiv:2405.03926v3). Yang et al. [10] model budget-constrained consensus and explicitly verify unilateral deviations after sequential updates. We adopt this separation of computation and verification without transferring their model-specific convergence results.

Drone routing studies include payload-dependent energy [11], uncertain demand and energy [12], and communication constraints [13]. These motivate studying scarce supporting infrastructure, but the present variables represent normalized reservation quantities. No payload, route, state-of-charge or radio model is embedded here. Cooperative facility location [14] and transportation cost allocation [15, 16] study coalition and fairness constraints, which differ from the unilateral deviations used in this paper.

2.1 Relationship to the authors' submitted UAV manuscript

A related manuscript by the authors, *UAV Scheduling under Triangular Uncertainty Energy Constraints and Coalition Stability*, has been submitted separately. That manuscript studies centralized sortie schedules, triangular orders, coalition costs, Shapley candidates and least-core repair. The present reconstruction studies

strategic continuous charging reservations, common-price equilibrium selection and aggregate/price computation. It uses no assignment, route, coalition value, theorem text, numerical table or figure from that manuscript. The elementary use of triangular descriptors and the application to drone operators are shared background. The related manuscript should be supplied confidentially to the editor with a comparison of scope; its unpublished status is not represented as a published reference.

3 Charging reservations with triangular preferences

Let $N = \{1, \dots, n\}$ index operators and $t = 1, \dots, T$ independent reservation periods. Operator i selects x_{it} with local upper limit $u_{it} > 0$. A common infrastructure operator announces capacity C_t, with $0 < C_t \le \sum_i u_{it}$. The shared feasible set is

$$K = \{x : 0 \le x_{it} \le u_{it}, \quad s_t := \sum_i x_{it} \le C_t \quad \forall t\}. \tag{1}$$

The local feasible set $K_i(x_{-i})$ is obtained by fixing competitors' reservations. Quantities are continuous and normalized. There is no integer charger assignment and no energy requirement coupling successive periods.

Let $a_{it} > 0$ penalize deviation from desired reservation $d_{it} \ge 0$. A triangular congestion descriptor is $\widetilde{\gamma}_{it} = (\gamma^\ell_{it}, \gamma^m_{it}, \gamma^u_{it})$, with $0 \le \gamma^\ell_{it} \le \gamma^m_{it} \le \gamma^u_{it}$. The three costs in period t are

$$f^e_{it}(x) = \tfrac{1}{2} a_{it}(x_{it} - d_{it})^2 + \gamma^e_{it} x_{it} s_t, \qquad e \in \{\ell, m, u\}. \tag{2}$$

Because $x_{it} s_t \ge 0$, these endpoints form a valid triangular cost. Membership grades describe the declared cost representation; they are not event probabilities.

Operator i declares positive, period-specific weights ω^e_{it} summing to one. The scalar objective and effective congestion coefficient are

$$f_i(x) = \sum_{t,e} \omega^e_{it} f^e_{it}(x) = \sum_t \left\{ \tfrac{1}{2} a_{it}(x_{it} - d_{it})^2 + k_{it} x_{it} s_t \right\}, \tag{3}$$

$$k_{it} = \sum_e \omega^e_{it} \gamma^e_{it} \ge 0, \qquad b_{it} = a_{it} d_{it}. \tag{4}$$

This is exactly a real-valued quadratic game once the weights are fixed. Positive scoring preserves endpoint improvements in the unilateral multiobjective comparison, but it does not recover all efficient choices or create a probability guarantee. Period-specific scores are applied before summation; they need not equal one common score of the summed triangle.

A GNE is a feasible x^* with $f_i(x^*) \le f_i(y_i, x^*_{-i})$ for every feasible unilateral y_i. Each local objective is strictly convex, with second derivative $a_{it} + 2k_{it} > 0$. We select the VE satisfying

$$\langle F(x^*), y - x^* \rangle \ge 0 \quad \forall y \in K, \qquad F_{it}(x) = (a_{it} + k_{it}) x_{it} + k_{it} s_t - b_{it}. \tag{5}$$

Here $F_{it} = \partial f_i / \partial x_{it}$ includes the effect of one's own reservation on s_t. The common multiplier interpretation is standard [1]. A VE is a GNE, but the reverse implication generally fails. Neither concept asserts coalition stability or equal welfare.

4 Aggregate and price characterization

Periods are independent, so suppress t. Put $D_i = a_i + k_i > 0$ and $[z]_0^{u_i} = \min\{u_i, \max\{0, z\}\}$. The KKT conditions for (5) are equivalent to

$$x_i = \left[\frac{b_i - k_i s - \lambda}{D_i}\right]_0^{u_i}, \quad s = \sum_i x_i \le C, \quad \lambda \ge 0, \quad \lambda(C - s) = 0. \tag{6}$$

The multiplier is common to the capacity constraint. Local bound multipliers are represented by clipping. Polyhedral normal cone calculus gives this equivalence without assuming monotonicity of F.

Theorem 1 (Capacity branches and unique allocation) *Define*

$$h(s) = \sum_i \left[\frac{b_i - k_i s}{D_i}\right]_0^{u_i} - s. \tag{7}$$

If $h(C) \le 0$, the unique root $s^0 \in [0, C]$ of $h(s) = 0$, together with $\lambda = 0$ and (6), gives the unique VE allocation. If $h(C) > 0$, every VE has $s = C$, and its allocation is obtained from any nonnegative root of

$$p(\lambda) = \sum_i \left[\frac{b_i - k_i C - \lambda}{D_i}\right]_0^{u_i} - C = 0. \tag{8}$$

Such a root lies in $[0, \max_i b_i]$. The primal allocation is unique in both cases; the capacity multiplier need not be unique.

Proof The function h is continuous and strictly decreasing: each clipped response is nonincreasing and the term $-s$ decreases strictly. Also $h(0) \ge 0$ and $h(\sum_i u_i) \le 0$. Therefore it has one root. If $h(C) \le 0$, this root is feasible and satisfies (6) with zero multiplier.

If $h(C) > 0$, no solution can have a slack capacity, since slackness would imply $\lambda = 0$ and require the infeasible root $s^0 > C$. For $s = C$, p is continuous and nonincreasing, $p(0) > 0$, and $p(\max_i b_i) = -C < 0$, so a root exists. The response at any root minimizes the strictly convex quadratic

$$\sum_i \{\tfrac{1}{2} D_i x_i^2 + (k_i C - b_i) x_i\} \quad \text{over } 0 \le x_i \le u_i, \ \sum_i x_i = C.$$

Thus all roots give the same primal allocation, even if a multiplier interval occurs when every component is at a bound. Finally, a positive multiplier cannot produce a saturated solution in the first branch with a different allocation: increasing λ cannot increase the response sum at $s = C$. If $h(C) < 0$ it is impossible, and if $h(C) = 0$ the same strict convexity argument gives the same allocation. These cases exhaust (6). □

The auxiliary quadratic in the proof freezes the equilibrium aggregate at C. It is not a social welfare objective for the original game. The theorem specializes aggregate response arguments [5] to this capped common-price selection.

4.1 Why a monotone pseudogradient is unnecessary here

For one period the Jacobian is $A = \operatorname{diag}(a + k) + k\mathbf{1}^\top$. Its symmetric part is

$$H = \operatorname{diag}(a + k) + \tfrac{1}{2}(k\mathbf{1}^\top + \mathbf{1}k^\top). \tag{9}$$

Strong monotonicity is sufficient for many standard VI algorithms but is not required by Theorem 1. For example, take $a = (0.1, 0.1)$, $b = (1, 1)$, $k = (0.01, 10)$, $u = (1, 1)$ and $C = 0.8$. The eigenvalues of H are approximately -1.063635 and 21.283635. Nevertheless, the theorem gives $x = (0.8, 0)$ and $\lambda = 0.904$. The objectives remain strictly convex in each player's own variable. Nonmonotonicity of F and local convexity are distinct properties.

The nonsymmetry of A also matters. Unless the k_i coincide, integrating F as if it were the gradient of an unweighted scalar potential changes the problem. Positive diagonal scaling can symmetrize some such games, but scaling the players' shared-constraint multipliers changes the VE selection. Our algorithm solves (5) with its original units.

4.2 Preference sensitivity on a fixed active set

Let J be the indices with $0 < x_i < u_i$ and let B denote the sum of fixed upper-bound allocations. Assume strict active set inequalities hold locally and vary only k_h for a free operator $h \in J$, keeping a, b, u, C fixed.

Proposition 2 (Local effect of a congestion coefficient) *In the slack branch, with* $E = 1 + \sum_{i \in J} k_i/D_i$,

$$\frac{\partial s}{\partial k_h} = -\frac{s + x_h}{D_h E}, \quad \frac{\partial x_j}{\partial k_h} = -\frac{k_j}{D_j}\frac{\partial s}{\partial k_h} \ (j \neq h,\ j \in J), \tag{10}$$

and

$$\frac{\partial x_h}{\partial k_h} = -\frac{s + x_h}{D_h}\left(1 - \frac{k_h}{D_h E}\right) < 0.$$

In the saturated branch let $W = \sum_{i \in J} 1/D_i$. *Then*

$$\frac{\partial \lambda}{\partial k_h} = -\frac{C + x_h}{D_h W}, \quad \frac{\partial x_j}{\partial k_h} = -\frac{1}{D_j}\frac{\partial \lambda}{\partial k_h} \ (j \neq h,\ j \in J), \tag{11}$$

and $\partial x_h/\partial k_h = -(C + x_h)D_h^{-1}(1 - (D_h W)^{-1}) \leq 0$. *Bound-fixed components have zero local derivative. These expressions apply away from active set changes.*

Proof In the slack branch, $s = B + \sum_{i \in J}(b_i - k_i s)/D_i$. Differentiate, using $\partial D_h/\partial k_h = 1$ and $(b_h - k_h s)/D_h = x_h$, to obtain (10). Differentiating each response gives the remaining formulas. The factor $k_h/(D_h E)$ is strictly less than one. In the saturated branch, differentiate $C = B + \sum_{i \in J}(b_i - k_i C - \lambda)/D_i$ to obtain (11). Here $D_h W \geq 1$, giving the weak sign for the own allocation. Fixed bound components do not vary until a bound changes status. □

Increasing upper-endpoint emphasis raises k_h when the corresponding score shift moves weight toward larger endpoint coefficients. The proposition describes this parameter effect, not a universal behavioral definition of risk aversion. Across active set boundaries the allocation remains continuous, while classical derivatives can change.

Algorithm 1 APB for one independent period

Require: $a > 0, b \geq 0, k \geq 0, u > 0$, $0 < C \leq \sum_i u_i$, update count q

Compute $D_i = a_i + k_i$ and $h(C)$
if $h(C) \leq 0$ **then**
    Bisect $h(s) = 0$ on $[0, C]$ for q updates
    Retain the upper bracket $\widehat{s}$ and set $\lambda = 0$
    $x_i \leftarrow [(b_i - k_i\widehat{s})/D_i]_0^{u_i}$
else
    Bisect $p(\lambda) = 0$ on $[0, \max_i b_i]$ for q updates
    Retain the upper bracket $\widehat{\lambda}$
    $x_i \leftarrow [(b_i - k_i C - \widehat{\lambda})/D_i]_0^{u_i}$
end if
Verify feasibility, common-price conditions and VI gap

4.3 A GNE certificate does not identify the VE

Example 1 Take two players, $a_i = 1$, $b_i = 10$, $k_i = 1$, $u_i = 1$ and $C = 1$. Every nonnegative allocation with $x_1 + x_2 = 1$ is a GNE: each player wants more than its residual capacity and cannot increase unilaterally. The unique VE is $(1/2, 1/2)$, with common multiplier 8. Thus vanishing unilateral regret alone cannot certify the selected common-price allocation.

5 Computation and verification

5.1 Aggregate and price bisection

We implement Theorem 1 as aggregate and price bisection (APB). The name describes the implementation; bisection itself is classical. The reference code performs 48 aggregate and 48 price updates on all periods in vectorized arrays, then retains the relevant branch. This fixed work avoids stopping choices based on observed outcomes. An implementation can skip the irrelevant branch in each period.

In exact arithmetic, either upper endpoint gives a capacity-feasible allocation. Each response evaluation costs $O(n)$, hence total work is $O(nTq)$ and storage $O(nT)$. The scalar bracket widths are at most $C_t 2^{-q}$ or $(\max_i b_{it})2^{-q}$. Since clipping is nonexpansive, the component allocation error is at most $(k_{it}/D_{it})C_t 2^{-q}$ in the aggregate branch and $(1/D_{it})(\max_i b_{it})2^{-q}$ in the price branch. Floating point roundoff must still be audited. This complexity statement assumes independent periods, a single unweighted shared capacity per period, and no additional local intertemporal constraints.

5.2 Certificates and independent checks

Feasibility is measured by the largest positive violation of (1). A natural VI residual is

$$r_{\mathrm{VI}}(x) = \|x - P_K(x - F(x))\|_\infty. \tag{12}$$

For a reported common multiplier λ, we additionally check $\|x - [x - F(x) - \lambda]_0^u\|_\infty$, $\lambda \geq 0$ and $\max_t |\lambda_t(C_t - s_t)|$. A separate linear optimization computes

$$g_{\mathrm{VI}}(x) = \max_{y \in K} \langle F(x), x - y \rangle. \tag{13}$$

It sorts the negative components of F in each period and fills the cheapest coordinates until capacity is reached. At a feasible point this gap is nonnegative and vanishes exactly at a VE, without a monotonicity assumption.

For unilateral verification, let $s_{-i,t} = s_t - x_{it}$ and $U_{it} = \min\{u_{it}, C_t - s_{-i,t}\}$. The exact best response is

$$y_{it}^{\mathrm{BR}} = \left[\frac{b_{it} - k_{it} s_{-i,t}}{a_{it} + 2k_{it}} \right]_0^{U_{it}}, \qquad r_{\mathrm{GNE}}(x) = \max_i \{ f_i(x) - f_i(y_i^{\mathrm{BR}}, x_{-i}) \}. \tag{14}$$

The implementation sums the regret over all periods for each operator before taking the maximum. A VE satisfies both checks, whereas Example 1 shows why a GNE need not.

For small problems we independently enumerate all lower/free/upper statuses and both capacity statuses, solve their linear complementarity systems, and reject candidates violating any sign or feasibility condition. This check does not use the aggregate root equations. The sorted-breakpoint projector used in (12) is separately compared with a constrained quadratic solver.

6 Completed synthetic experiments

6.1 Design and reproducibility

All inputs, result files, code, logs, environment details and figure-generation scripts are included in Online Resource 1, the companion reproducibility archive. The studies were executed for this reconstruction on 6 November 2026. None of the thirty historical assignment instances or operational schedules from the related UAV manuscript is reused.

For n operators and T periods, draw independent $a_{it} \sim U[1.5, 3.5]$, $d_{it} \sim U[0.8, 1.8]$ and $u_{it} \sim U[0.8, 1.6]$. Let

$$m_{it} = \frac{v_{it} \exp(\eta Z_{it})}{n}, \quad v_{it} \sim U[0.3, 1], \quad Z_{it} \sim \mathcal{N}(0,1), \quad \widetilde{\gamma}_{it} = (0.6 m_{it}, m_{it}, 1.8 m_{it}). \tag{15}$$

Weights follow Dirichlet$(2,2,2)$ and $C_t = \rho \sum_i u_{it}$. Unless specified otherwise, $\eta = 0.6$ and $\rho = 0.45$. The $1/n$ factor keeps the scale of aggregate congestion comparable as population size grows. These are constructed preference descriptors, with no fitted membership function or claim of empirical uncertainty calibration.

The environment is Python 3.12.2, NumPy 2.3.2 and SciPy 1.18.1 on macOS 14.6.1, ARM. BLAS thread limits are set to one before importing NumPy. Wall times use a monotonic performance counter, exclude generation and external audits, and include the actual solver calls. Each path is warmed up and timed three times; the median

Table 2 Completed study blocks and prespecified seed families

Study	Size and count	Seeds/settings
Active set validation	$n = 4, T = 1$; 90 cases	$2026110600 + r$, $0 \le r < 30$; $\rho \in \{0.2, 0.6, 1\}$
Scaling APB versus EG	Five sizes, six cases each, $T = 6$	$n \in \{8, 32, 128, 512, 2048\}$; $2026111000 + 10n + r$
KKT comparison	Three sizes, six cases each, $T = 1$	$n \in \{8, 32, 128\}$; $2026114000 + 10n + r$
GNE selection	$n = 16, T = 6$; 30 cases	$2026112000 + r$; $\eta = 1, \rho = 0.45$
Preference and capacity audits	$n = 16, T = 6$; 30 base cases	$2026115000 + r$; $\eta = 1$; recorded capacity variants
Capacity curve	$n = 8, T = 6$; 18 capacities	2026113000; ρ evenly spaced from 0.15 to 1

is retained per instance. These subsecond timings are implementation measurements, not cross-platform complexity estimates.

6.2 Independent correctness validation

All 90 active set cases agree with APB to a maximum component difference of 7.78×10^{-15}. Thirty independent random projections agree with SciPy SLSQP quadratic projections to 4.89×10^{-15}. Across the thirty scaling inputs, APB has maximum natural residual 4.80×10^{-14} and maximum raw VI gap below 1.00×10^{-10}. The nonmonotone two-player example has a negative smallest eigenvalue as stated above and natural residual 3.17×10^{-14}. These checks support implementation consistency with the theorem; finite samples do not replace its proof.

6.3 Comparison on the same selected equilibrium

The extragradient (EG) implementation uses the classical two-projection iteration [17], $y = P_K(x - \alpha F(x))$, $x^+ = P_K(x - \alpha F(y))$. It starts at zero and uses $\alpha = 0.8/L$, where

$$L = \max_t \{\max_i (a_{it} + k_{it}) + \sqrt{n}\|k_{\cdot t}\|_2\}$$

is a valid Lipschitz upper bound. Its projector uses sorted breakpoints rather than a general optimization subroutine. The stopping threshold is $r_{\mathrm{VI}} \le 10^{-7}$, checked every five iterations, with a limit of 20000 iterations. APB uses 48 updates per scalar branch and exceeds this requested accuracy. All tested EG runs meet the threshold in 65–80 iterations; convergence is recorded empirically for these inputs, without applying a monotone-VI theorem to the nonmonotone stress example.

Table 3 and Fig. 1 show that APB benefits from replacing repeated projections by scalar response sums. Its median paired speed ratio over EG increases from about 25.7 at eight operators to 44.3 at 2048 operators. The largest case contains 12288 continuous decisions. This advantage is specific to a model that admits independent

Table 3 Same-game computation with six periods and six instances per size. Time is the median of the retained per-instance wall times. Speed is the median paired EG/APB ratio

n	APB (ms)	EG (ms)	Speed	Max EG residual
8	0.717	18.460	25.7	7.71e-08
32	0.752	19.809	26.0	8.23e-08
128	1.031	26.890	25.8	9.50e-08
512	2.017	66.273	32.8	9.88e-08
2048	5.830	257.705	44.3	9.95e-08

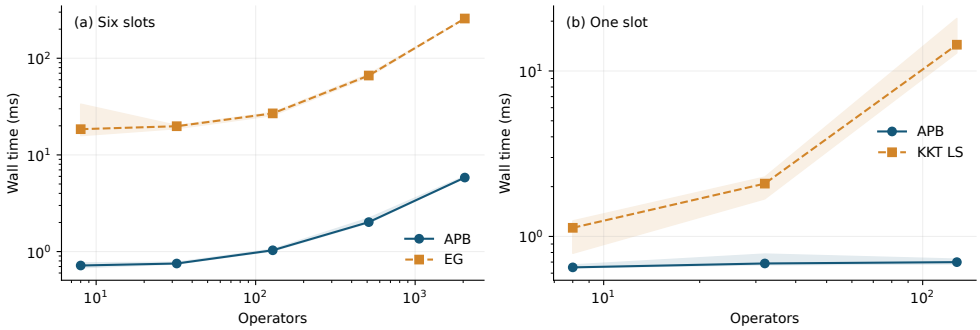

Fig. 1 Wall time on identical games in each comparison panel, with per-instance median times summarized by their median and shaded minimum to maximum range across six inputs; the panels use different numbers of periods

scalar branches; it does not compare APB with specialized compiled water-filling implementations or with the full range of modern GNE solvers.

We also implement a KKT least squares baseline using SciPy `least_squares`, analytic piecewise Jacobians, box stationarity residuals and a Fischer–Burmeister capacity complementarity equation. Tolerances are 10^{-12} and the evaluation limit is 500. Its role is to compare two implementations of the same common-price system; it is not the published NashOpt implementation [3]. All eighteen cases pass 10^{-7} natural residual. At eight operators its small absolute times make the speed comparison particularly sensitive to overhead.

6.4 Capacity and preference effects

Fig. 2 follows one archived eight-operator input through eighteen capacity ratios. Requested quantity increases until the unconstrained aggregate fits; the common multiplier then becomes zero. This is the branch transition established analytically, not a fitted relationship. The six periods transition at potentially different capacities.

Preference comparisons retain all inputs and replace the effective congestion coefficient by heterogeneous scores, modes, centroids or upper endpoints. For thirty inputs

Table 4 Separate one-period KKT comparison with six inputs per size and median paired KKT/APB speed ratios

n	APB (ms)	KKT LS (ms)	Speed
8	0.650	1.128	1.7
32	0.687	2.086	3.0
128	0.700	14.412	21.0

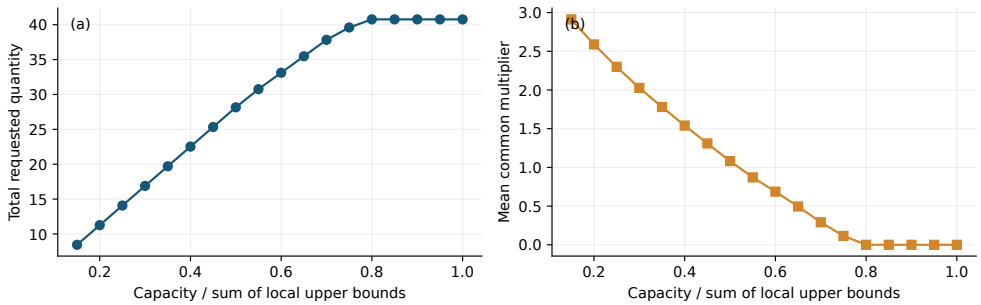

Fig. 2 A capacity sweep on one fixed input showing total reservations and the mean capacity multiplier across six independent periods

Table 5 Mean preference effects over thirty identical base inputs at capacity ratio 0.8. RMS compares allocations with the heterogeneous VE; cross-game regret is evaluated using the heterogeneous objectives

Preference	Quantity	Mean price	RMS change	Cross-game regret
Heterogeneous	80.042	0.0089	0.0000	2.7e-15
Modal	82.041	0.0137	0.0672	0.205
Centroid	79.933	0.0081	0.0600	0.13
Upper	71.116	0.0004	0.1470	0.739

with $\rho = 0.8$ and $\eta = 1$, Table 5 and Fig. 3 report resulting quantities and changes from the heterogeneous VE. A policy change defines a different game and is not an algorithm comparison. Regret evaluated in the heterogeneous game makes this distinction visible. The upper descriptor gives a larger congestion coefficient and lower average requested quantity, but this is not evidence of greater empirical reliability or better welfare.

An additional finite-difference audit increases the first operator's k by 10^{-5} in each period at $\rho \in \{0.25, 0.8, 1\}$ over thirty base inputs. All ninety variants have nonincreasing own reservations, nondecreasing competitors' reservations and nonincreasing

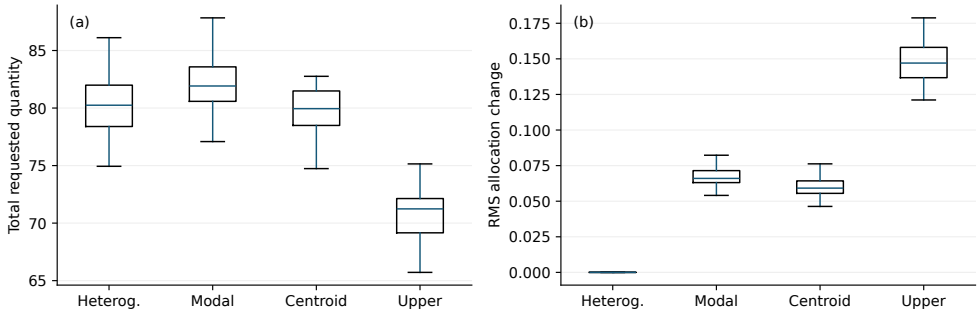

Fig. 3 Distributions across thirty inputs for total quantity and RMS change under each declared preference; boxes show quartiles and medians and whiskers extend to 1.5 interquartile ranges

aggregate demand within 10^{-9}. This numerical sign check includes bound transitions, while Proposition 2 states the local differentiable formulas.

To expose the role of the capacity constraint, an ablation computes the VE after replacing C_t by $\sum_i u_{it}$, then evaluates it against the original $\rho = 0.25$ capacities. All 180 periods across thirty inputs are overloaded. The per-instance maximum relative overload has mean 2.096 and range 1.855–2.590. These figures quantify violation in a deliberately constrained synthetic generator; they do not estimate infrastructure demand in a real depot.

6.5 Sequential best responses select different GNEs

For thirty inputs with $\rho = 0.45$ and $\eta = 1$, sequential exact best responses start at zero in forward and reverse operator orders. Updates stop at 10^{-10} in maximum coordinate change, with at most 10000 sweeps. The maximum unilateral regret is below 4.0×10^{-15} for reverse updates and below 4.2×10^{-16} for forward updates. Yet the mean raw VI gaps are approximately 111.5 and 112.2, respectively; maximum natural residuals exceed 1.59. The mean RMS differences from the VE are 0.506 and 0.513. These outputs are valid GNEs to the checked tolerance, but they do not solve the selected VE problem. Fig. 4 illustrates the resulting reservation patterns on one input. This experiment is a selection comparison rather than a claim that sequential methods fail to compute a GNE. It also explains why comparing only runtime or unilateral regret across differently selected equilibria can be misleading.

7 Discussion and conclusions

For the specified game, a common-price allocation can be found through either aggregate consistency at zero multiplier or price clearing at capacity. The characterization establishes existence and uniqueness of the primal VE, including parameters for which the full pseudogradient is nonmonotone. The explicit sensitivity formulas separate reduction in an operator's own reservation from redistribution to competitors. Independent enumeration, direct deviation checks and a VI gap make these mathematical distinctions computationally visible.

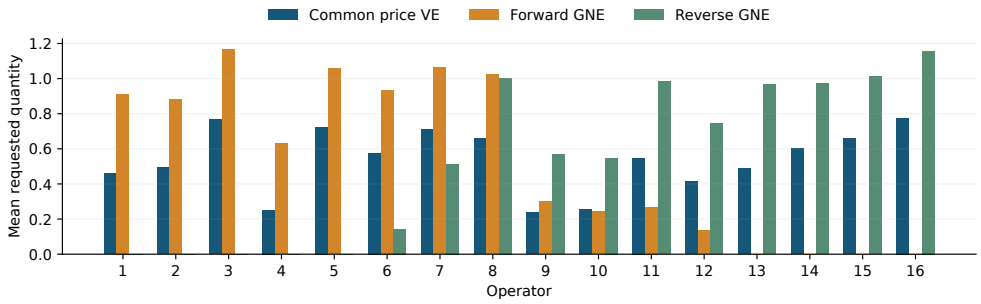

Fig. 4 Mean reservations per operator across six periods in one archived input, comparing the VE with forward and reverse sequential best response outcomes

The completed experiments support an implementation advantage over the two reported local baselines, under shared data and a common equilibrium target. They do not establish superiority over all GNE algorithms. Aggregate reduction is classical, the quadratic objective is a restricted model, and adding triangular descriptors does not itself supply an original algorithm. The research value lies in the complete capped characterization, preference analysis and auditable experiment design; assessment of its incremental novelty should include the close aggregative and resource allocation literature [5, 6].

The model is best read as strategic reservation analysis for infrastructure associated with drone fleets. Independent periods exclude battery state transitions, minimum energy requirements, charger switching, queue dynamics and mission deadlines. The weights and triangular coefficients are synthetic, and their behavioral meaning requires calibration. Adding intertemporal energy requirements or heterogeneous capacity coefficients generally destroys the scalar branch structure and calls for a more general VI or complementarity method. No claim is made about feasible aircraft schedules, physical flight performance or coalition defection.

Declarations

Data availability. The datasets generated during and/or analysed during the current study are available from the corresponding author on reasonable request.
Ethics. The study involves no human participants or animals.

References

[1] Kulkarni AA. Games and teams with shared constraints. Philos Trans R Soc A. 2017;375:20160302. https://doi.org/10.1098/rsta.2016.0302

[2] Dreves A, Kanzow C. Nonsmooth optimization reformulations characterizing all solutions of jointly convex generalized Nash equilibrium problems. Comput Optim Appl. 2011;50:23–48. https://doi.org/10.1007/s10589-009-9314-x

[3] Bemporad A. NashOpt: a Python library for computing generalized Nash equilibria. Optim Methods Softw. 2026;41:732–753. https://doi.org/10.1080/10556788.2026.2661736

[4] Corchón LC. Aggregative games. SERIEs. 2021;12:49–71. https://doi.org/10.1007/s13209-021-00229-5

[5] Itaya J, von Mouche P. Equilibrium uniqueness in aggregative games: very practical conditions. Optim Lett. 2022;16:2033–2058. https://doi.org/10.1007/s11590-021-01780-7

[6] Harks T, Timmermans V. Equilibrium computation in resource allocation games. Math Program. 2022;194:1–34. https://doi.org/10.1007/s10107-020-01604-z

[7] Costa TM, Osuna-Gómez R, Chalco-Cano Y. New preference order relationships and their application to multiobjective interval and fuzzy interval optimization problems. Fuzzy Sets Syst. 2024;477:108812. https://doi.org/10.1016/j.fss.2023.108812

[8] Urbanec T. Linearity and linear extensions of fuzzy orders revisited. Fuzzy Sets Syst. 2024;480:108876. https://doi.org/10.1016/j.fss.2024.108876

[9] Lampariello L, Sagratella S, Sasso VG. Addressing hierarchical jointly convex generalized Nash equilibrium problems with nonsmooth payoffs. SIAM J Optim. 2025;35:445–475. https://doi.org/10.1137/23M1574026

[10] Yang J, Zhu X, Li YW, Lin GH, Dutta B, Martínez L. Non-cooperative maximum utility consensus under limited budgets: a generalized Nash equilibrium and regulation mechanism. Fuzzy Optim Decis Mak. 2026;25:571–609. https://doi.org/10.1007/s10700-026-09486-0

[11] Cheng C, Adulyasak Y, Rousseau LM. Drone routing with energy function: formulation and exact algorithm. Transp Res B. 2020;139:364–387. https://doi.org/10.1016/j.trb.2020.06.011

[12] Chagas GO, Coelho LC, Laganà D, Beraldi P. A dynamic drone routing problem with uncertain demand and energy consumption. Transp Res B. 2025;202:103335. https://doi.org/10.1016/j.trb.2025.103335

[13] Cicek CT, Koç Ç, Gultekin H, Erdoğan G. Communication-aware drone delivery problem. IEEE Trans Intell Transp Syst. 2024;25:9168–9180. https://doi.org/10.1109/TITS.2024.3371189

[14] Liu L, Gong Z. Coalition-based facility location optimization for urban UAV logistics. Transp Res C. 2026;186:105624. https://doi.org/10.1016/j.trc.2026.105624

[15] Chen S, Wang H, Meng Q. Cost allocation of cooperative autonomous truck platooning: efficiency and stability analysis. Transp Res B. 2023;173:119–141. https://doi.org/10.1016/j.trb.2023.04.008

[16] Lu W, Quadrifoglio L. Fair cost allocation for ridesharing services: modeling, mathematical programming and an algorithm to find the nucleolus. Transp Res B. 2019;121:41–55. https://doi.org/10.1016/j.trb.2019.01.001

[17] Korpelevich GM. The extragradient method for finding saddle points and other problems. Matecon. 1976;12:35–49. English translation. https://cs.uwaterloo.ca/~y328yu/classics/extragrad.pdf